Available online at www.sciencedirect.com
SCIENCE DIRECT®
Physica C 405 (2004) 240–244
PHYSICA C
www.elsevier.com/locate/physc

Observation of nonuniform current transport in epitaxial $YBa_2Cu_3O_{7-x}$ film near the superconducting transition temperature

L.B. Wang [a], M.B. Price [a], J.L. Young [a], C. Kwon [a,*], Timothy J. Haugan [b], Paul N. Barnes [b]

[a] *Department of Physics and Astronomy, California State University Long Beach, 1250 Bellflower Boulevard, Long Beach, CA 90840, USA*

[b] *Air Force Research Laboratory, 2645 Fifth Street, WPAFB, OH 45433-7919, USA*

Received 15 December 2003; received in revised form 16 January 2004; accepted 11 February 2004
Available online 12 March 2004

Abstract

We have studied the local transport properties in an epitaxial $YBa_2Cu_3O_{7-x}$ (YBCO) film on $LaAlO_3$ (LAO) using variable temperature scanning laser microscope (VTSLM) near the superconducting transition. A map of the superconducting transition temperature (T_c^*) is generated from a series of VTSLM images. The map of T_c^* indicates there are inhomogeneities in the film large enough to create nonuniform current flow near the superconducting transition. The evaluated T_c^* varies between 90.3 and 91.0 K in the film. Even though such change in T_c^* is not large enough to be detected by other localized compositional and structural characterization techniques, this along with an area of lower T_c^* and/or higher resistance affects current flow near the superconducting transition temperature as shown in VTSLM images. This inhomogeneity may be caused by slight variations of the stoichiometry and/or oxidation of the YBCO film.

PACS: 74.62.–c; 74.72.Bk; 74.76.Bz
Keywords: YBCO film; Inhomogeneity; T_c; Variable temperature scanning laser microscopy

1. Introduction

High temperature superconducting (HTS) cuprate oxides have been extensively studied to understand the fundamental properties of these materials as well as to develop various power and device applications. The complex crystal structure of cuprate oxides can lead to substantial spatial inhomogeneity complicating the situation. Hence, spatially resolved studies of HTS are of scientific and technological importance both to evaluate the general quality of the samples and to determine local values of important parameters.

In conventional transport measurements of superconducting samples, the measured quantities such as critical current densities and critical temperatures are averaged over the whole sample and do not reflect the local distribution of the

* Corresponding author. Tel.: +1-562-985-4855; fax: +1-562-985-7924.
E-mail address: ckwon@csulb.edu (C. Kwon).

0921-4534/$ - see front matter © 2004 Elsevier B.V. All rights reserved.
doi:10.1016/j.physc.2004.02.003

quantities. Due to the complex materials chemistry and structure, many kinds of inhomogeneity can be created in HTS and the global properties measured by conventional measurement techniques are susceptible for those inhomogeneities. Hence, numerous techniques have been developed and utilized for spatially resolved studies of HTS. Magneto-optic imaging is used to visualize the superconducting screening current in ceramic YBCO [1] and YBCO coated conductor [2]. Hall-probe magnetometry is employed to study current-carrying properties of melt-textured YBCO–YBCO junction [3]. Near-field microwave microscope is developed to study the local nonlinear response of a YBCO bi-crystal junction [4]. Scanning SQUID microscopy is used to measure the current distribution and the Josephson penetration length in YBCO [5,6].

More direct measurement techniques to study local variations of superconducting properties in HTS are the hot-spot scanning method such as low temperature scanning electron microscopy (LTSEM) [7] and low temperature scanning laser microscopy (LTSLM) [8–10]. Earlier our group reported the observation of the spatial distribution of the superconducting transition temperature T_c using variable temperature scanning laser microscopy, which measures the response due to the laser hot-spot near the superconducting transition [11–13].

In this paper, we report a spatial map of the superconducting transition temperature (T_c^*) generated from a series of VTSLM images in an YBCO epitaxial film. Although the film has higher $T_c(R = 0\ \Omega) = 90.1$ K with a narrow superconducting transition width (0.7 K), we still detect the inhomogeneous distribution of superconducting transition temperature, which creates the inhomogeneous current flow in the film. This inhomogeneity may have been caused by a slight variation of stoichiometry and/or oxidation.

2. Experimental

The YBCO film was produced by pulsed laser deposition described in detail elsewhere [14,15]. The laser used was a LPX 300 series model Lambda Physik excimer laser operating at the KrF, 248 nm, wavelength. YBCO was ablated onto a LAO(1 0 0) single crystal substrate. The oxygen deposition pressure was 300 mTorr kept constant in the chamber using a downstream throttle-valve control as O_2 gas flowed into the chamber during growth. Substrates were attached to the heater using a thin layer of colloidal Ag paint and heated to ~785 °C. After deposition, films were cooled in O_2 for post-deposition oxygenation.

The film size was 2 mm wide and 7 mm long. To determine the thickness, kapton was applied to the YBCO layer exposing only a portion of the film. The exposed portion was etched with a 4% solution of nitric acid (seen in Fig. 3(a) as the white portion on the upper and lower section of the film). The thickness of the YBCO film was determined to be 230 nm using multiple profilometry measurements across the acid etched step edges. The temperature dependence of the film resistance was measured by a four-probe technique. Gold was deposited on the surface of the film, and platinum wires were soldered on the gold spots by indium. AC susceptibility measurements were also performed on the film [16].

For VTSLM measurements, a 5.2 mW helium–neon laser beam (wavelength 632.8 nm) modulated at 1 kHz by a standard mechanical chopper is coupled into an optical fiber and focused on the surface of the film by a lens. The fiber and lens assembly is fastened to a three-axis movable stage system which scans the laser beam on the surface of the film in both horizontal and vertical directions. The ac voltage data were acquired by a lock-in technique using a lab-edited Labview program. The ac voltage data was transformed into image by commercial software. The temperature of the film was controlled by a cryogenic system of cryostat and a temperature controller. The detailed experimental setup can be found in previous reports [11–13,17].

3. Results and discussion

Fig. 1 shows the temperature dependence of resistance, the inset is an enlargement of the

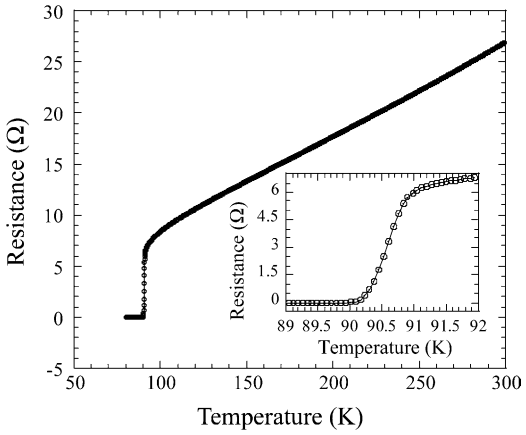

Fig. 1. The temperature dependence of resistance of the film. The bias current is 5 mA.

transition region. From the R vs. T curve, the film has T_c ($R = 0\ \Omega$) of 90.1 K with a 0.7 K transition width. Fig. 2 is a plot of the ac susceptibility curves, χ'' vs. T where χ'' is the imaginary part of the loss component. A similar transition width of ~0.7 K is apparent from the lowest, 0.025 Oe, magnetic field line data. This indicates that the film is quite homogeneous. However, one notices double peaks in 0.025 Oe data indicative of two different $T_c s$ in the film. We have observed the inhomogeneous $T_c s$ in the film from a series of VTSLM images.

Fig. 3 is a film photograph and images of VTSLM measurements at different temperatures. Corresponding to the photograph of the film, the boundaries of the film in the images are indicated by arrows. The strong signals occur at the edge of

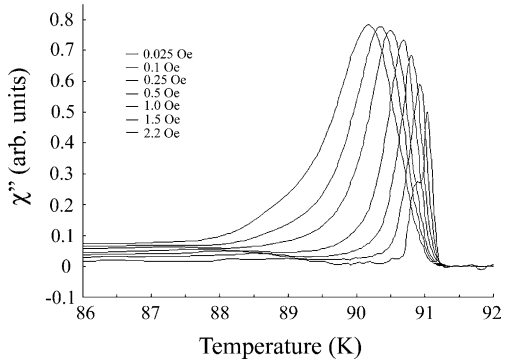

Fig. 2. AC susceptibility data for the film.

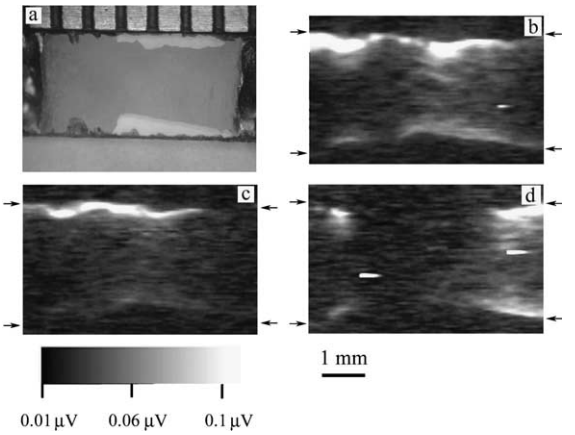

Fig. 3. The photograph of the film and the images from the VTSLM measurements. Arrows indicate the region of the film. The bias current is 5 mA. (a) The photograph of the film, (b) 90.8 K, (c) 90.6 K, (d) 90.3 K.

the film with the variation of temperature. In the images from VTSLM, the signals δV can be approximately expressed by

$$\delta V = j_b(x,y)\frac{\partial \rho(x,y)}{\partial T}\Lambda \delta T \tag{1}$$

where δV is ac voltage signal, $j_b(x,y)$ local current density, $\frac{\partial \rho(x,y)}{\partial T}$ the derivative of resistivity with respect to temperature, Λ the disturbed area due to the laser beam, δT the increase in temperature due to heating caused by the laser beam, respectively [18]. Since a VTSLM image is a plot of $\delta V(x,y,T)$, $\delta V(T)$ has a peak when $\frac{\partial \rho(x,y)}{\partial T}$ is the maximum. We define T_c^* as the temperature where $\delta V(T)$ is a maximum.

Fig. 4 shows the temperature dependent δV at a certain position. Fixing the laser beam at a certain position and slowly increasing temperature, the temperature dependent δV is measured and plotted as solid triangles. With the variation of temperature, δV reaches its maximum value, δV_m, at a temperature which is defined as T_c^*. Data is also taken from the previously acquired images at the same position and included as solid circles in Fig. 4. The temperature dependent measurement of δV and $\delta V(T)$ taken from VTSLM images at the same position show good agreement. As such, it is apparent that VTSLM measures the local superconducting transition $\frac{\partial \rho(x,y)}{\partial T}$ vs. T.

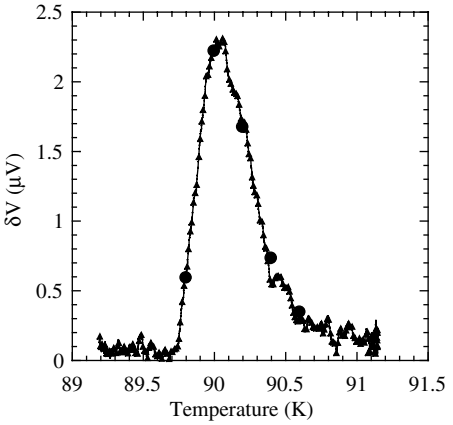

Fig. 4. The temperature dependence of δV and δV data from images. The bias current is 5 mA. Solid triangles are data from measurement of δV and solid circles are δV data from images.

A program was developed to select the $T_c^*(x,y)$ and $\delta V_m(x,y)$, the maximum value of δV, from a series of VTSLM images taken at a range of temperatures in order to find the spatial distribution of δV_m and T_c^*. This program interpolates δV data at different temperatures for a given position of the film and evaluates δV_m and T_c^* at the point. By applying this interpolation throughout the film, a distribution of δV_m and T_c^* in the film can be mapped. A noise level threshold was chosen such that any data not exceeding that threshold would be zero. When this data is fitted by the program, the temperature difference between the fitted peak and measured peak is about ±0.1 K. Fig. 5 is a distribution of δV_m and T_c^* obtained from the program.

In Fig. 5(a), the large δV_m mainly occurs at the edges of the film, while some areas inside the film have a δV_m lower than the noise level as shown in black. The evaluated T_c^* in Fig. 5(b) indicates spatial nonuniformity of about 0.6 K, which is detectable by VTSLM, but is quite small. The spatial variation of T_c^* reflects the variation of T_c ($R = 0\ \Omega$). δV_m is related to the local current density as shown in Eq. (1). When the film is wider than the beam diameter, the nonuniform current transport $j_b(x,y)$ may well be caused by the T_c^* variation in the film as well as the spatial distribution of $\rho(x,y)$. As such, it is possible to consider the local variation of current while assuming that $j_b(x,y)$ does not change with temperature.

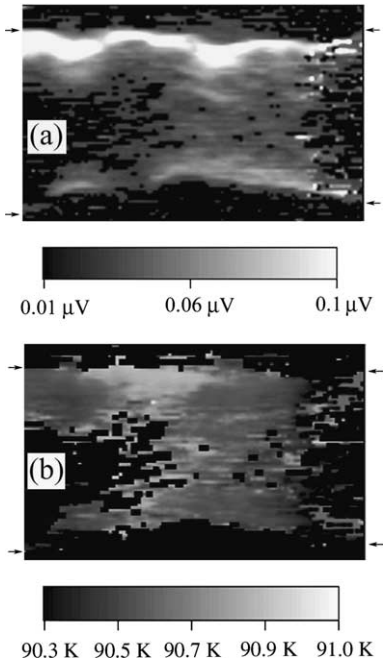

Fig. 5. The distribution of δV m and T_c^*. (a) δV m (V), (b) T_c^* (K). Arrows indicate the region of the film.

In general, the maximum of $\frac{\partial \rho(x,y)}{\partial T}$ is assumed to be the same at every location on the film; Λ and δT are also almost constant [18]. Hence, δV_m will be approximately proportional to $j_b(x,y)$ according to Eq. (1). In Fig. 5(a), the large δV_m mainly occurs at the edges of the film. This indicates that there is a larger current density at the edges and the current mainly flows along the edges. The upper edge has a stronger signal than the bottom edge indicating that there is more current flowing along the upper edge than the bottom edge. In the middle of the film, there are some dark areas which cannot be evaluated since their signal is lower than the noise level threshold. In these dark areas, less current is flowing. From Fig. 5(b), the variation of T_c is quite small in the evaluated areas about 0.6 K. Even though the difference of T_c is small, the nonuniform distribution of T_c still creates percolative current paths.

Usually, T_c will change with composition and structure [19,20]. An attempt was made to detect localized compositional and structural abnormalities that would correlate with the change in T_c by

material characterization techniques, but none was observed. However, since the difference in T_c is so small, the change of local composition and structure would be quite small and may not observable except by high resolution techniques. If minute compositional and structural defects are indeed present, they are still sufficient to affect current flow near the superconducting transition temperature. It is quite possible that the inhomogeneity is caused by slight variations in the stoichiometry and/or oxidation of the YBCO film.

4. Conclusion

In summary, an epitaxial YBCO film on LAO was studied by VTSLM. This film shows great uniformity in temperature dependence of the resistance. However, VTSLM measurements indicate that there are still inhomogeneities in this film. Even though the inhomogeneity of T_c is very small, it creates a nonuniform current distribution especially near the critical transition temperature. This inhomogeneity may be caused by slight variations in the stoichiometry and/or oxidation of the film. Detection of these minute variations in the local composition and structure will require high resolution techniques. Such nonuniformity near the critical transition temperature can affect the critical current and microwave properties in these regions, also.

Acknowledgements

This work was supported by the Air Force Office of Science Research under grant no. F49620-01-1-0493. AC susceptibility measurements were provided by Iman Maartense, a UDRI contractor for the Air Force Research Laboratory.

References

[1] J. Albrecht, Ch. Jooss, R. Warthmann, A. Forkl, H. Kronmüller, Phys. Rev. B 57 (1998) 10332.
[2] D.M. Feldmann, J.L. Reeves, A.A. Polyanskii, G. Kozlowski, R.R. Biggers, R.M. Nekkanti, I. Maartense, M. Tomsic, P. Barns, C.E. Oberly, T.L. Peterson, S.E. Babcock, D.C. Larbalestier, Appl. Phys. Lett. 77 (2000) 2906.
[3] G. Karapetrov, V. Cambel, W.K. Kwok, R. Nikolova, G.W. Crabtree, H. Zheng, B.W. Veal, J. Appl. Phys. 86 (1999) 6282.
[4] S.-C. Lee, S.M. Anlage, Appl. Phys. Lett. 82 (2003) 1893.
[5] J.W.H. Tsai, S.W. Chan, J.R. Kirtley, S.C. Tidrow, Q. Jiang, IEEE Trans. Appl. Supercon. 11 (2001) 3880.
[6] A. Sugimoto, T. Yamaguchi, I. Iguchi, Physica C 357 (2001) 1473.
[7] D. Kölle, F. Kober, M. Hartmann, R. Gross, R.P. Heubener, B. Roas, L. Schultz, G. Saemann-Ischenko, Physica C 167 (1990) 79.
[8] A.G. Sivakov, A.V. Lukashenko, D. Abraimov, P. Muller, A.V. Ustinov, M. Leghissa, Appl. Phys. Lett. 76 (2000) 2597.
[9] N. Dieckmann, A. Bock, U. Merkt, Appl. Phys. Lett. 68 (1996) 3626.
[10] T. Kiss, M. Inoue, S. Egashira, T. Kuga, M. Ishimaru, M. Takeo, T. Matsushita, Y. Iijima, K. Kakimoto, T. Saitoh, S. Awaji, K. Watanabe, Y. Shiohara, IEEE Trans. Appl. Supercon. 13 (2003) 2607.
[11] S. Seo, C. Kwon, B.H. Park, Q.X. Jia, Mat. Res. Soc. Symp. Proc. 689 (2002), E8.22.1.
[12] L.B. Wang, M.B. Price, C. Kwon, Q.X. Jia, IEEE Trans. Appl. Supercon. 13 (2003) 2611.
[13] C. Kwon, L.B. Wang, S. Seo, B.H. Park, Q.X. Jia, IEEE Trans. Appl. Supercon. 13 (2003) 2894.
[14] T. Haugan, P. Barnes, I. Maartense, L. Brunke, J. Murphy, Physica C 397 (2003) 47.
[15] T.J. Haugan, P.N. Barnes, R.M. Nekkanti, I. Maartense, L.B. Brunke, J.P. Murphy, Mat. Res. Soc. Symp. Proc. 689E (2002) 217.
[16] I. Maartense, A.K. Sarkar, J. Mater. Res. 8 (1993) 2177.
[17] B. Klein, Thesis, California State University, USA.
[18] R. Gross, D. Koelle, Rep. Prog. Phys. 57 (1994) 651.
[19] R.J. Cava, B. Batlogg, C.H. Chen, E.A. Rietman, S.M. Zahurak, D. Werder, Phys. Rev. B 36 (1987) 5719.
[20] E. Osquiguil, M. Maenhoudt, B. Wuyts, Y. Bruynseraede, Appl. Phys. Lett. 60 (1992) 1627.